

PERIODICO di MINERALOGIA
established in 1930

*An International Journal of
MINERALOGY, CRYSTALLOGRAPHY, GEOCHEMISTRY,
ORE DEPOSITS, PETROLOGY, VOLCANOLOGY
and applied topics on Environment, Archaeometry and Cultural Heritage*

Microcracking of granite feldspar during thermal artificial processes

David Martín Freire-Lista^{1,2,*}, Luz Stella Gomez-Villalba¹ and Rafael Fort^{1,2}

¹ Instituto de Geociencias IGEO (CSIC, UCM) Spanish Research Council
CSIC, Complutense University of Madrid UCM, Madrid, Spain

² CEI Campus Moncloa, UCM-UPM and CSIC, Madrid, Spain

*Corresponding author: d.freire@igeo.ucm-csic.es

Abstract

Granite is one of the most widely used building stone and is a main component in many heritage buildings for its austere appearance and its availability as a stone of the Earth's crust. When exposed at the Earth's surface, thermal changes are responsible for its decay, especially in granites exposed to weathering. Feldspars, an important component of granite mineralogy, are among the most likely crystalline phases susceptible to microcracking, which, in turn, causes the disintegration of crystals lattices. Microcracks generated in granite feldspars during thermal processes such as freeze-thaw and thermal shock cycles, carried out in the laboratory, were studied to understand the decay process of granite buildings. The aim of this study is to determine microcrack propagation (both as inter- and intra-crystalline microcracks types) within feldspars (potassium feldspars and plagioclases) of two building granites located near the city of Madrid (Spain). Potassium feldspars and plagioclases developed different mechanisms of microcracking, probably, due to their microstructures and/or driven, preferentially, by crystallographic anisotropies such as twinning and zoning of the precursor mineral, and neoformation of secondary mineral phases at the expense of a primary mineral phase. By combining petrographic analysis of the studied granite stones, with physical laboratory tests (thermal shock and freeze-thaw tests), we outlined the evolution of microcracking in order to identify the potential problems that disintegration may cause to stone monuments and buildings.

Key words: physical disintegration; feldspars; thermal shock; freeze-thaw; building stone; decay; weathering.

Introduction

Feldspar minerals are abundant in most of the building stone used since the oldest Egyptian monuments. Granite is used as a building stone in façades, walls, dados of buildings, bases of large structures, statues, fountains, milestones and paving worldwide (Vazquez et al., 2010; Pires, 2014) as well as Egyptian temples and obelisks, which remain among the largest stone monuments in history (e.g., Iversen, 1992). This building stone may be subject to temperature changes that produce decay (Gomez-Heras et al., 2006, 2008, 2009; Sousa, 2014) outlined the factors affecting durability of building granite stone, they depend mostly on extrinsic factors such as environmental, (e.g. temperature changes) and intrinsic conditions such as mineralogy, pre-existing microcracks and microstructure (Schouenborg, 1996; Reuschlé et al., 2003; 2006) defined by compositional zoning, twins, dislocations, deformation bands or cleavage, among others. Feldspars, potassium feldspars (K-Fsp) and plagioclases (Pl) have easier microcrack propagation by their two perfect cleavage systems (Tullis and Yund, 1985; 1987; 1992; Hadizadeh and Tullis, 1992). Microcracks produced by freezing water (Ingham, 2005; Takarli, et al., 2008; Freire-Lista et al., 2015a) are due to the combination of several mechanisms including the volumetric expansion of water during freezing (Ozcelik et al., 2012), hydraulic pressure (Hor and Morihiro, 1998), and ice segregation (Walder and Hallet, 1985; Akagawa and Fukuda, 1991; Hallet et al., 1991; Matsuoka and Murton, 2008). The microcracks caused by thermal shock are due to volumetric expansion of the stone minerals (Lin, 1995, 2002; Franzoni et al., 2013; Hall and Thorn, 2014; Vázquez et al., 2015). Therefore, the thermal expansion coefficient of each mineral will define the thermal decay and anisotropies within each crystal. At temperatures below 400° C, the plagioclase has a higher thermal expansion

coefficient than K-feldspar (Skinner, 1966).

Propagation of microcracks (Kranz, 1983; Åkesson et al., 2004; Malaga-Starzec et al., 2006; Anders et al., 2014) in granite stone (Íñigo et al., 2000, 2013; Tan et al., 2011) due to thermal changes (Chen et al., 2008; Bayram, 2012; Inserra et al., 2013; Jamshidi et al., 2013) is an aspect that should be taken into account when assessing decay of granites used as building stone (Garcia-del-Cura et al., 2008).

The aim of this work is to characterize the decay induced by physical weathering in the K-feldspars and plagioclases crystal microstructures due to thermal changes (freeze-thaw and thermal shock). Microcrack propagation, in turn, promotes chemical weathering both in building stones as in natural rocks with felsic plutonic character (e.g., Le Pera and Sorriso-Valvo, 2000; Wilson, 2004; Scarciglia et al., 2005; Caracciolo et al., 2012; Scarciglia et al., 2012), feldspars (Page and Wenk, 1979; Eggleton and Buseck, 1980).

There are few studies on physical weathering processes caused by thermal fluctuations that affect K-feldspar and plagioclase microstructures, and in this regard, our study will help in understanding the granite stone microfabric in equivalent environmental conditions.

Materials and methods

Rock samples

The behavior of two granites used in the building heritage in Spain, Alpedrete granite (hereinafter AL) and Zarzalejo granite (hereinafter ZA) has been investigated.

Both stones are extracted from quarries located in plutons belonging to the Guadarrama Batolite, in the southwest of the Sierra de Guadarrama, in the eastern part of the Spanish Central System (Villaseca et al., 1998; Villaseca and Herreros, 2000) Granites are formed by plutonic complex intrusion (Brandebourger, 1984) during the Carboniferous-Lower Permian. Granites correspond to an acid magmatism, average

composition “monzogranite” late to post-orogenic and belong to the province of *Piedra Berroqueña* (Fort et al., 2011; Freire-Lista and Fort, 2015) with a continental Mediterranean climate and with a medium precipitation value of 384 mm/year.

The Alpedrete pluton (350 km²) has many historical quarries near to its core and is located approximately 45 km north of the city of Madrid (Fort et al., 2010). Alpedrete granite is an equigranular, medium- to fine-grained monzogranite (Freire-Lista et al., 2015a).

The blocks, from which samples have been cut, were taken from an historic granite quarry,

located in Alpedrete village (40°39'45.7"N - 4°00'47.7"W) (Figure 1). This granite has been widely used as building stone for important heritage buildings, for example the Royal Palace (1735-1764) in Madrid (Fort et al., 2013). Alpedrete granite has been nominated as a Global Heritage Stone Resource due to its heritage importance (Freire-Lista et al., 2015b).

The Zarzalejo pluton is located about 60 km northwest of the city of Madrid. Two types of granites can be differentiated by their texture: a porphyritic texture characterized by the occurrence of K-feldspar megacrystals with medium-grained crystals and an equigranular granite (López-Arce et al., 2010). In this work, an equigranular with medium to coarse crystal size was tested. This granite has been widely used, e.g. Royal Monastery at El Escorial (1563-1584). Samples were taken from an historic granite quarry (40°32'15.97"N - 4°10'26.89"W) geologically located within the margins of the Zarzalejo pluton (Figure 1).

The tectonic history of the two granites is similar and both granites are slightly deformed. The petrophysical properties of Alpedrete and Zarzalejo granites are presented in Table 1.

Testing

Thermal shock test (TS test). 7 cubes corresponding to AL and ZA granite samples ($5 \times 5 \times 5 \pm 0.5$ cm) were used for performed 42 test cycles according to European standard EN 14066, 2003. First, the samples were put in a ventilated oven at 105 ± 5 °C for 18 h. Samples were taken from the oven and then put into water at room temperature for 6 h. When TS cycle is up to the 42 cycles, the TS test ended.

Freeze-thaw test (FT test). FT testing was conducted as specified in European standard EN 12371, 2001 (with 280 cycles). 7 cubes ($5 \times 5 \times 5 \pm 0.5$ cm) of Alpedrete and Zarzalejo granite samples were water-saturated at 20 °C and atmospheric pressure for 48 ± 2 h. The samples

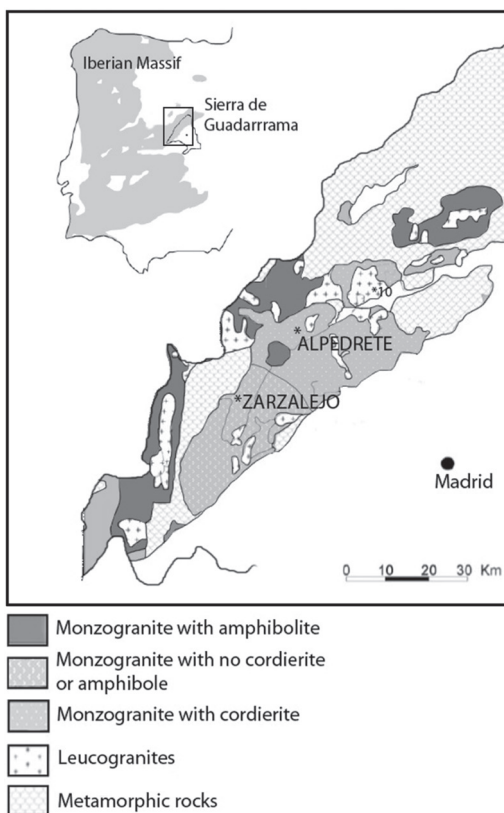


Figure 1. Location map of Alpedrete and Zarzalejo granites. After Fort et al., 2013.

Table 1. Relationship of physical properties for Alpedrete granite and Zarzalejo granite.

Property	Alpedrete granite	Zarzalejo granite
Impact strength (cm)	68 ± 14 ⁽¹⁾	58.8 ⁽²⁾
Compression strength (Mpa)	136.9 ± 41 ⁽¹⁾	160.0 ± 49.0 ⁽²⁾
Flexural strength (Mpa)	8.88 ± 3.69 ⁽¹⁾	8.21 ± 2.25 ⁽²⁾
Bulk density (Kg/m ³)	2636 ± 10 ⁽³⁾	2657 ± 15 ⁽³⁾
Young's Modulus (MPa)	33275 ⁽³⁾	26882 ⁽³⁾
Water absorption (%)	0.3 ± 0.0 ⁽⁴⁾	0.6 ± 0.0 ⁽⁴⁾
Water saturation (%)	0.5 ± 0.2 ⁽²⁾	1.24 ⁽²⁾
Capillary absorption coefficients (g·m ⁻² ·s ^{-0.5})	1.523 - 3.1983 ⁽⁴⁾	4.238 - 4.796 ⁽³⁾
Porosity accesible to water (%)	0.8 ± 0.1 ⁽³⁾	1.7 ± 0.06 ⁽⁵⁾
Mercury intrusion porosity (%)	0.44 ⁽³⁾	1.4 ⁽³⁾
Frost resistance (%)	0.01 ⁽¹⁾	0.005 ⁽²⁾
Ultrasonic P-wave velocity propagation (m/s)	4625 ± 163 ⁽³⁾	3219 ± 204 ⁽³⁾
Ultrasonic S-wave velocity propagation (m/s)	3812 ± 92 ⁽³⁾	$2\ 2116 \pm 89$ ⁽³⁾
Total anisotropy (%)	5.8 ⁽⁵⁾	12.7 ⁽⁵⁾

Note: ⁽¹⁾ Menduiña and Fort, 2005; ⁽²⁾ Bernabeu et al., 2004; ⁽³⁾ Freire-Lista et al., 2015a; ⁽⁴⁾ Fort et al., 2011; ⁽⁵⁾ Fort et al., 2013.

were subsequently placed in an air-filled FT test chamber (dry conditions), where they were spaced no less than 10 mm apart and at least 20 mm from the side of the chamber. The temperature sequence in each 12 h cycle was as follows: (i) the temperature was lowered from + 20 to 8 °C in 2 h (dry conditions); (ii) and then to 12 °C in 4 h (dry conditions); (iii) the chamber was automatically filled with water in 0.5 h until the specimens were completely submerged at temperatures of

5 to 20 °C (wet conditions); (iv) the specimens remained submerged for 5 h; and (v) the water in the chamber was emptied in 0.5 h.

The FT chamber was fitted with a control system that allows programming the FT cycles to an accuracy of ± 1.0 °C.

X-Ray Diffraction. Representative samples from both granites, Alpedrete and Zarzalejo, were selected for X-Ray diffraction (XRD)

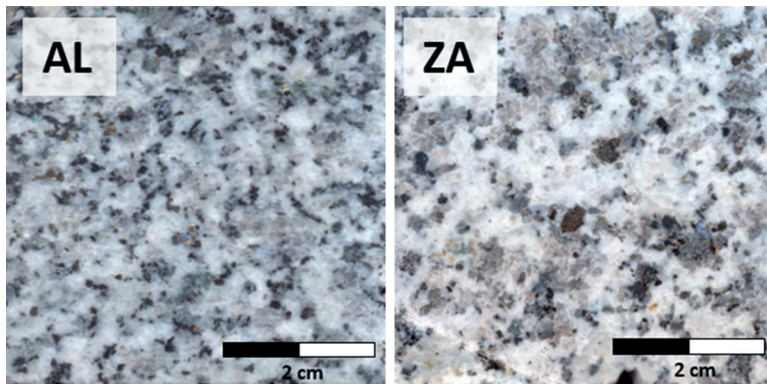


Figure 2. Hand samples. AL: Alpedrete granite, ZA: Zarzalejo granite.

analyses. With this technique, the mineralogical phases and the possible preferential orientations associated can be detected. The sample was ground manually and some quartz crystals were separated and removed to minimize its high reflectance power and a ground fraction < 50 mm was obtained. A Phillips PW-1710 Cu K α radiation powder diffractometer was used, and the scanning conditions were 2 θ angles of 2 - 68°, scan step size 0.02°, scanning rate 2°/min in continuous mode, and beam intensity of 40 kV

and 30 mA. The software PCPDFWIN was used for comparing the results with the referenced in the JCPDS database (Joint Committee on Powder Diffraction Standards).

Fractography. Thin sections of $30 \times 20 \pm 3$ mm with a thickness of 30 μ m were made from the cuts of one specimen (Williams et al., 1958; Mills, 1991) of the Alpedrete and Zarzalejo granites before and after 280 FT test cycles and 42 TS test cycles.

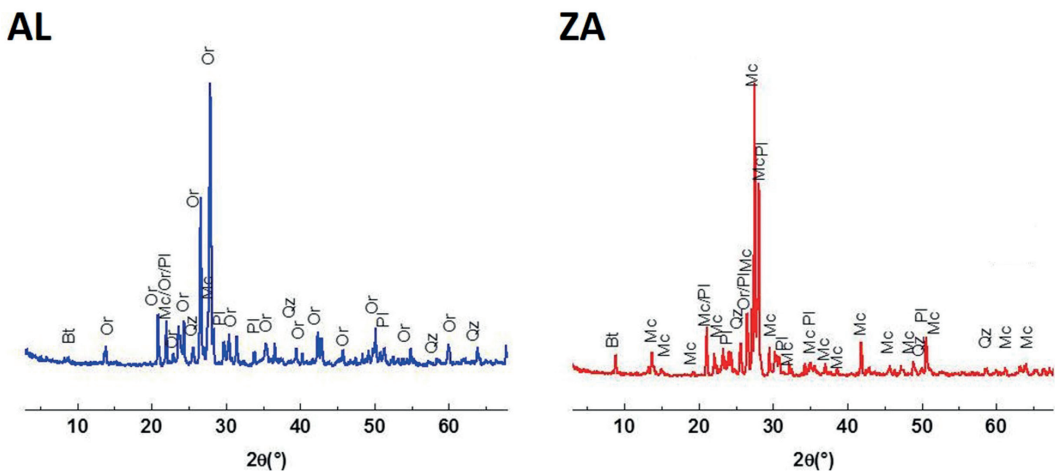


Figure 3. XRD patterns of Alpedrete (AL) and Zarzalejo (ZA) granites. Biotite (Bt), quartz (Qz), microcline (Mc), plagioclase (Pl), orthoclase (Or).

These thin sections have been cut into the parallel faces of the specimens to ensure the propagation of microcracks observation of the same family. Sawing was performed at low speed (120 rpm) and low strain so as not to generate microcracks. The thin sections were stained with sodium cobaltonitrite to better discriminate K-feldspar from plagioclase.

All thin sections have been impregnated with fluorescein according to Sousa et al. (2005) and characterised under an Olympus BX 51 polarized light microscope (PM) fitted with DP 12-coupled (6 V/2.5 Å) Olympus digital micrography and Olympus DP-Soft software (version 3.2). Microcracks were characterised with the same equipment, as well as with the same set-up using an Olympus U-RF-T mercury lamp fluorescence microscope (FM).

The Michel-Lévy method was used to determine the composition of plagioclase in thin sections (Michel-Lévy, 1894).

Fluorescein is rapidly deteriorated when the thin section is also stained with sodium cobaltonitrite, so it is necessary to carry out the petrographic analysis immediately after staining.

Polarized light and fluorescence micrograph mosaics were made from the thin sections to study before and after the FT and TS tests microcracks. Each mosaic comprised about 40 micrographs, measuring approximately 4.5 cm² of each thin section. The cross-nicols micrograph mosaics were used for mineral quantification and the fluorescence mosaics to study microcracks. Each fluorescence micrograph mosaics was laid over the same area of the polarized light crossed nicols micrograph mosaics and on the resulting micrograph mosaics was drawn a rectangle (1 × 2 cm) divided into 5 × 5 mm squares (A total of 110 mm, linear). The sides of this mesh were drawn parallel to the two sides of the original cubic specimens.

The volume of K-feldspar and plagioclase and number of microcracks which intersects

the sides of this mesh has been measured, considering the microcracks that cut across K-feldspars and plagioclases. Intercrystalline and intracrystalline microcracks have been differentiated in each mineral phases.

Results

X-Ray Diffraction (XRD)

In Alpedrete granite (AL) sample the typical pattern of orthoclase (JCPDS = 75-1190) records the highest intensity peak as 220 (26.9°) and the second in intensity to 002 (27.5°).

In low signal, peaks can be assigned to sodic plagioclase (Pl, $a = 8.1350 \text{ Å}$, $b = 12.7840 \text{ Å}$, $c = 7.1594 \text{ Å}$, space group: C-1), microcline (Mc, $a = 8.5714 \text{ Å}$, $b = 12.9645 \text{ Å}$, $c = 7.2203 \text{ Å}$, space group: C-1), biotite (Bt, $a = 5.357 \text{ Å}$, $b = 9.255 \text{ Å}$, $c = 20.23 \text{ Å}$, space group: C 2/c) and quartz (Qz, $a = 4.913 \text{ Å}$, $c = 5.405 \text{ Å}$, space group: P3₂21 or P3₂21).

In Zarzalejo granite sample (ZA), the predominant phase is microcline (8.5714 Å, $a = b = c = 7.2203 \text{ Å}$ 12.9645 Å, space group: C-1), although peaks with low intensity correspond to orthoclase (Or), sodium plagioclase (Pl), quartz (Qz) and biotite (Bt). shows the results of XRD analyzes performed on a selection of feldspar occurring in both samples, Alpedrete and Zarzalejo granites.

Petrographic results

Alpedrete granite (AL) before thermal tests. AL granite has the texture of granite, holocrystalline, hypidiomorphic, granular with the typical plagioclase-quartz-potassium feldspar paragenesis (Figure 4) plagioclase is presented in oligoclase type subhedral crystals (An 28-30), being slightly alkaline at the edges (An 11-15). In general plagioclase develops albite-carlsbad twin (1-4 mm), zoning (0.1-3.5mm) and polysynthetic twins (1.8-4 mm). Quartz occupies irregular interspaces (1.5-3.5 mm). The feldspar is orthoclase (around 1.5-4.5 mm),

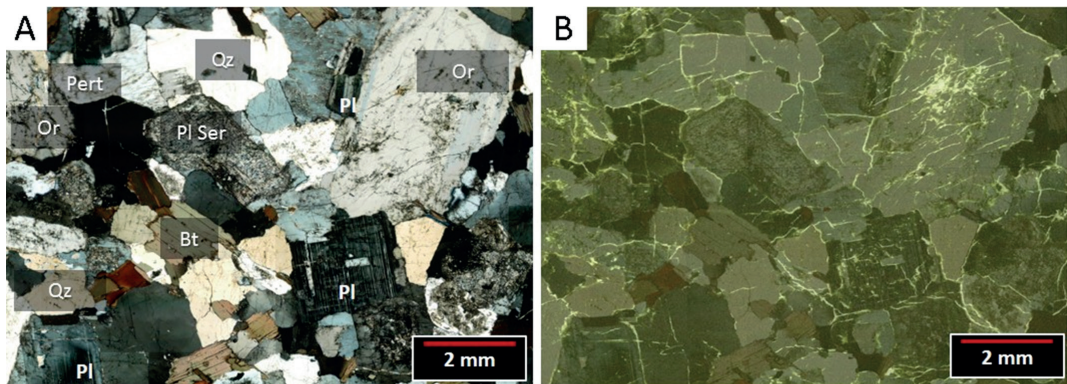


Figure 4. General aspect of the Alpedrete sample before the treatments showing the hypidiomorphic-granular texture. Biotite sheets (Bt), quartz (Qz), Orthoclase (Or), plagioclase (Pl), perthite (Pert) and sericite (Ser). A: Polarized light micrograph mosaic, crossed nicols. B: Fluorescence micrograph mosaic overlaid on polarized light micrograph mosaic.

usually kaolinized and with perthite textures. Perthite crystals (~ 0.3 mm wide) are arranged at the edges where the plagioclase becomes more alkaline. Laminar crystals of biotite (0.8-1.7 mm) are presented randomly distributed throughout the sample.

A detail of the texture in the fresh rock is shown in Figures 4a and 4a'. In this case, locally perthites are aligned with twin planes; the fracturing affects such the orthoclase crystals which are arranged in an uneven pattern and the polysynthetic twins with displacement of 0.19 mm. Besides occasionally slightly bent polysynthetic twins are observed. In the center, sericitized plagioclase is aligned with biotite sheets showing typical zircon inclusions and dark halos around the zircon (Figure 5d). A detail in Figure 5d shows albite lamellae present within microcline forming perthite textures, biotite richer in iron with inclusions of pleochroic halos around zircon.

Several generations of biotite have been identified in the fresh rock; the earlier in flakes, the following occupying cracks and veins, which generally produce alterations to iron oxide (Figure 5c), and the later presented superimposed to the veins (Figure 5a). Details

of the microcracks of about 0.1 mm thickness occur and are filled with clay minerals are shown in Figure 5a. These are arranged cutting the feldspars. The microcracking affects several feldspars, forming subparallel sinuous branches with separation of 0.25 mm. The veins are filled with phyllosilicates or iron oxides: these later are formed by weathering as precipitates along biotite cleavage planes and microcracks (Figure 5c). Other biotite crystals (0.5-1.2 mm) are not aligned with microcracks which happened in a post-fracturing process (Figure 5a). Throughout these microcracks are aligned twinning planes of euhedral plagioclase crystals. Inside them multiple microcracks are distributed at angles of 35° with the twin plane (Figure 5c).

Zarzalejo sample (ZA) before thermal test. ZA sample before the thermal treatments, shows a typical holocrystalline hypidiomorphic granular texture (Figure 6). It consists mainly of intermediate composition plagioclase (An 38-40) associated with orthoclase, microcline and quartz. The K-feldspar (K-Fsp) is subhedral whereas crystals of quartz (Qz) are anhedral. Two regions are observed in the image (Figure 6). The inside region, which shows orthoclase

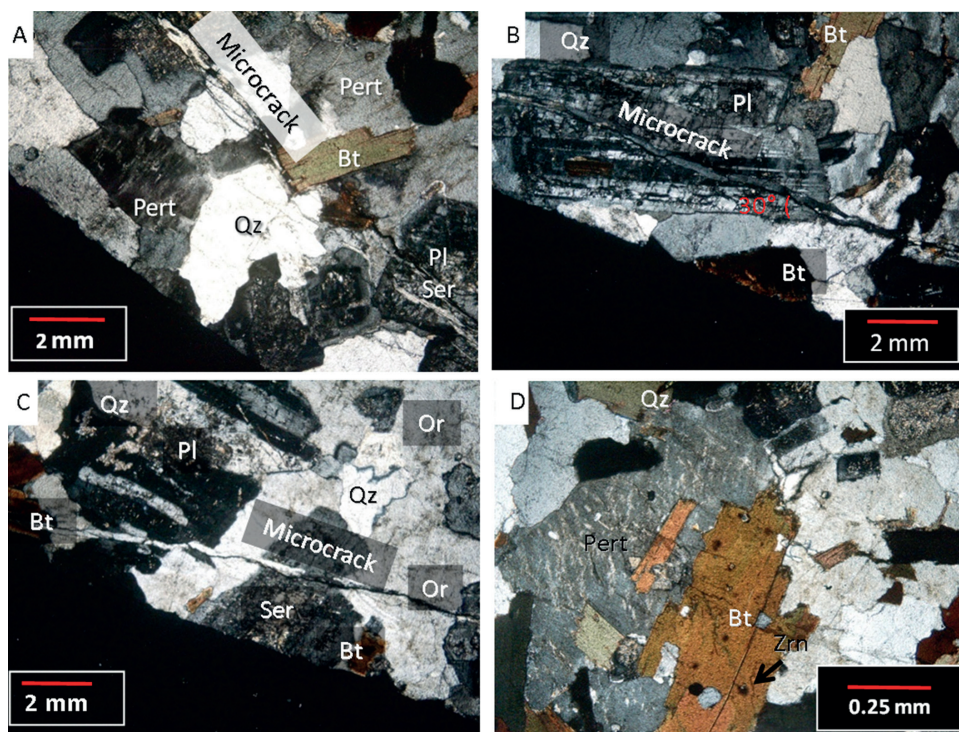


Figure 5. Polarized light micrograph of Alpedrete sample before the treatments, crossed nicols. Biotite (Bi) Orthoclase (Or), plagioclase (Pl), perthite (Pert), sericitized plagioclase (Ser) and quartz (Qz) affected by microcracking. A: A sheet of biotite is over the microcrack. B: Microcrack affecting a plagioclase with polysynthetic twinned. C: Microcracking with filling of phyllosilicates and iron oxides affecting the original texture. D: Detail showing perthites, biotite with zircon, quartz and K feldspar.

in association with intermediate plagioclase (An 38) and quartz. In this area are common perthites, microcline-perthite crystals and plagioclase with sericitization (Ollier, 1983) due to volatile-rich residual solutions that induce alterations, so that pre-existing minerals, (as in the plagioclase) are veined or replaced by new ones (Williams et al., 1958). The outer region, the crystals are slightly smaller, predominantly polysynthetic or zoned twinned plagioclase (about 1.5-2.6 mm) with a predominant alkaline composition (An 26), whose microcracks occasionally are filled with smaller chloritized biotite (about 1.3 mm) (Figure 6). In this case the chlorite occurs replacing biotite along rims and lamellae and

has been observed in a later stage of biotite weathering (Borelli et al., 2012; Stoch and Sikora, 1976; Ollier, 1983). The chloritization might have occurred under relatively oxidizing conditions (Tabbakh Shabani, 2009). In detail, the core of the image shows a larger crystal of orthoclase (around 10 mm). There is a marked tendency for elongated minerals like biotite sheets (1.4 mm), twin planes in orthoclase and plagioclase (individual or polysynthetic) to be aligned more or less parallel with their major axes, so as to produce a determined lineation. However, in the case of occasional biotites which are perpendicular to the main alignment have a tendency to be folded according to this direction.

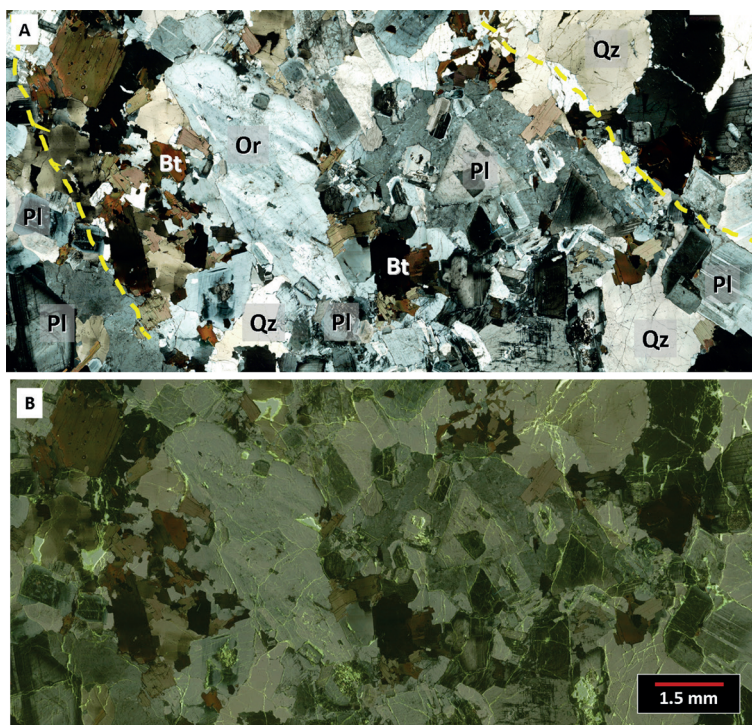


Figure 6. General aspect of the Zarzalejo granite showing the hypidiomorphic granular texture with two regions delimited by discontinuous lines. The inner region shows a big orthoclase crystal (Or) associated to plagioclase (Pl), quartz (Qtz) and biotite (Bt). There is a tendency to be aligned the twin planes of plagioclase with the orthoclase, biotite sheets have a tendency to be folded according the same orientation. The outer region shows smaller crystals of plagioclase at left or bigger crystals of quartz at right. A: Polarized light micrograph mosaic, crossed nicols. B: Fluorescence micrograph mosaic overlaid on polarized light micrograph mosaic.

Inside the big K-feldspar, microcracks were developed generally arranged in an uneven pattern. However, there is a predominance of microcracks sub-perpendicular to the direction of the greater length of the crystal, and other sub-parallel to the greater length (Figure 6). Throughout these microcracks have aligned perthite patterns, as well quartz inclusions and plagioclase crystals (0.4 mm) aligned with the major axis.

These alignments suggest different stages of crystallization, one before when the alkaline feldspars (including potassium and sodium feldspars) and accessory minerals as micas

were formed followed for a stage where a reorientation occurred, affecting only the inner region.

An enlargement of Figure 6 shows subhedral crystals of plagioclase (Pl, 1.8 mm) associated with subhedral and anhedral crystals of orthoclase (Or, 0.9-2.5 mm) locally developing Albite-Carlsbad and microcline-perthite twins.

Crystals appear as polysynthetic twins (An 34-38) which are aligned with lenticular exsolution lamellae of plagioclase (Figure 6, center) and microcline-perthite crystals. Locally exsolved plagioclase is cut by microcline veins of 1.3 mm. The microcline twinning is

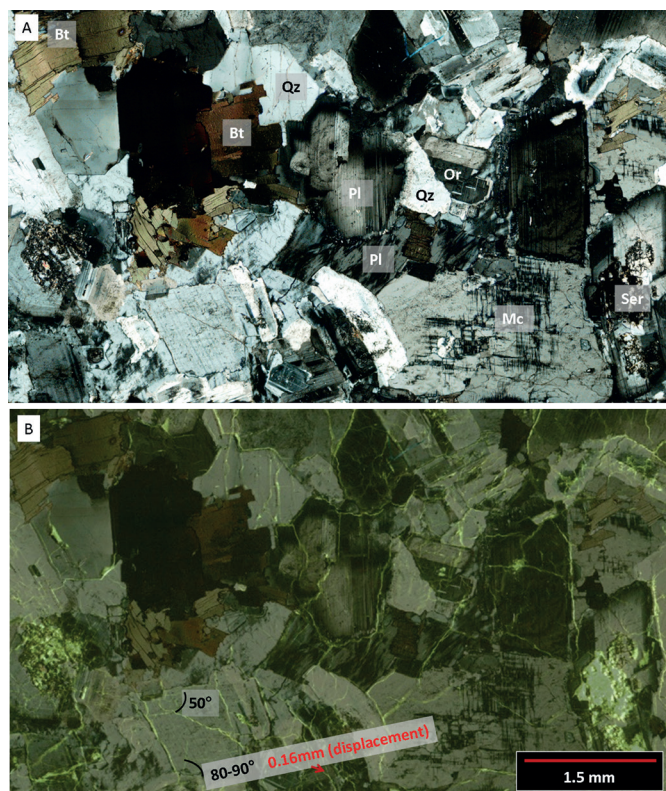


Figure 7. Plagioclase associated to orthoclase (Or) and microcline (Mc). Polysynthetic twins are aligned with lenticular exsolution lamellae of plagioclase (Pl) (In the center). Sericitization process within plagioclase crystals (Ser) and details of microcracks. A: Polarized light micrograph mosaic, crossed nicols. B: Fluorescence micrograph mosaic overlaid on polarized light micrograph mosaic showing the microcracking.

most intense adjacent to plagioclase lamellae and has crystallographic continuity with twin planes. This disposition could be result of stage of corrosion and filling by slightly different relationship Na/Ca of Plagioclase (Smith, 1974). In the bottom right of the Figure 7, well-developed tartan twinning microcline (around 2.2 mm) with quartz inclusions (0.1-0.3 mm) are observed. In the top left, sheet crystals of biotite (around 0.4-0.7 mm) are mainly oriented parallel to twinning planes. Zircon is included in biotite, developing dark metamictic halos around it. In the bottom, individual crystals are internally affected by microcracks. In the left an

orthoclase crystals (0.7 mm) is locally affected by microcracks with angle of 50° or 70°. Besides, zig-zag microcracks are present forming angles of 80-90° with respect to twinning planes or surfaces fractured in an uneven pattern affecting only the crystals inner. Pre-existent stacking fault planes produce local displacement around 0.2 mm affecting the polysynthetic twins. Sericitization are observed in the inner of some plagioclase crystals.

Petrographic results after thermal tests. In both granites, the thermal processes increased the size of pre-existing open microcracks

and facilitated the development of new microcracks. Microcracks propagated mostly by microstructural planes at nearly orthogonal cleavage, compositional zoning, twins and K-feldspar and plagioclase boundaries. Thus, Figure 8 (AL) shows microcracks in plagioclase cores (marked in red) with porosity. These pores increased considerably after the treatments. Another common microcracking propagation plane is at perthite boundaries, as seen in Figure 8 (ZA). The right side shows how the microcracks propagate along cleavage planes 001 and 010.

Quantification of microcracks. Alpedrete granite has fewer pre-existing microcracks than Zarzalejo granite as Figure 9 shows. Inter- and intracrystalline microcracks have proliferated in both granitic samples. The TS test increased the microcracks in both granites faster than FT test.

Intracrystalline plagioclase microcracks are more abundant at the end of FT and TS tests

in Al sample. However, in ZA sample, the largest number of intracrystalline microcracks occurred in K-feldspar crystals.

Discussion

The physical decay induced by FT and TS tests generates feldspar microcracks. Clay minerals are formed as a by-product of the plagioclase degradation in granites, which become more susceptible to weathering. This occurs because the alkaline ion content in the water increases gradually with time (Suzuki et al., 1995). The penetration of water and air pollution in contact with the granite surface is facilitated by inter- and trans-crystalline microcracks. These microcracks act as pathways that accelerate chemical weathering of minerals that produce decay.

The petrographic description is representative of these granites, but not exhaustive, due to local changes in the sampling zones. Factors such as local fault regions, environmental

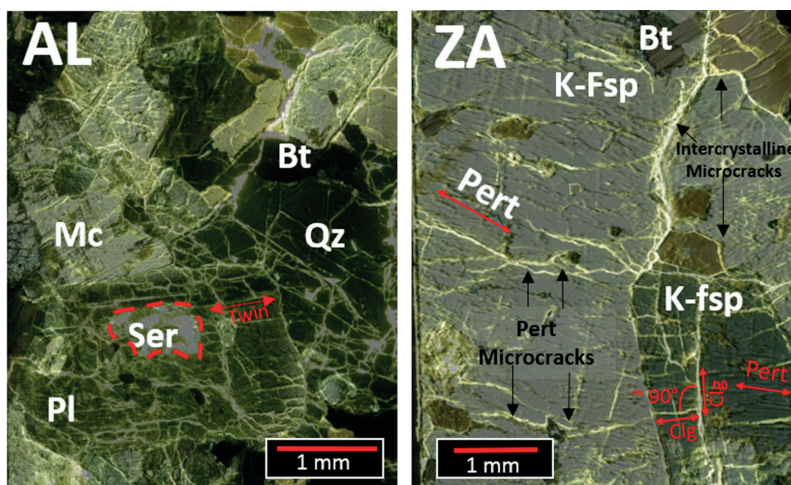


Figure 8. Fluorescence micrograph overlaid on polarized light micrograph. Alpedrete granite (AL) after 42 TS cycles and Zarzalejo granite (ZA) after 280 FT cycles. Plagioclases (Pl), Potassium feldspar (K-Fsp) perthites (Pert), microcline (Mc) and microcracks in cleavage (Clg). Biotite group (Bt), sericitization processes in plagioclase (Ser) and details of microcracks.

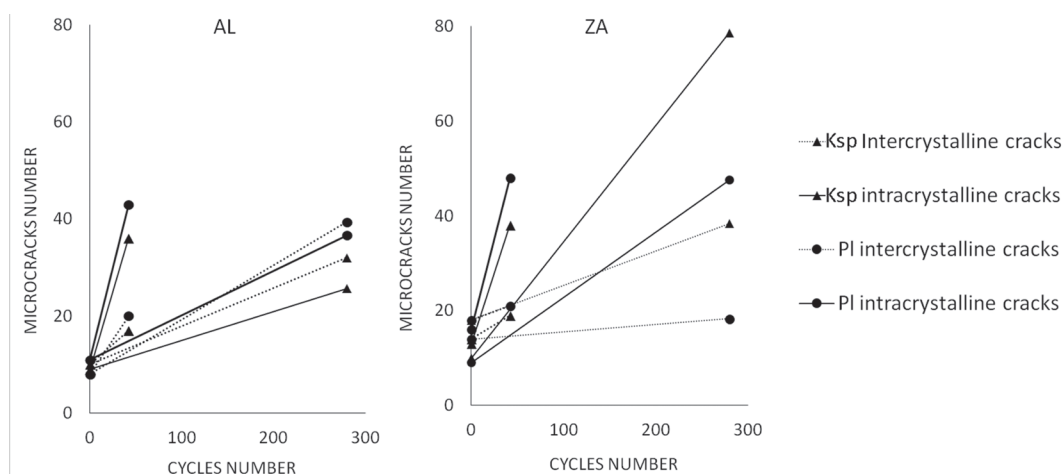


Figure 9. Number of internal microcracks (dotted line) and intracrystalline (solid line) affecting plagioclase (PI) (circles) and k-feldspar (Ksp) (triangles) in Alpedrete granite (AL) and Zarzalejo granite (ZA) for 280 cycles of freeze-thaw (FT) test and 42 thermal shock cycles (TS) test.

conditions including climatic factors (Heins, 1995), geological factors, such as the position in the pluton, either near the margins or the cores are reflected in the texture or mineralogical changes. This is the case of Alpedrete granite placed closer to the pluton core and Zarzalejo granite placed on the pluton margins. In any case, thermal, tectono-thermal or tectonic history (Bard, 1986) could modify this behaviour, implying fracturing or alteration which modify the granite durability, as deduced from the tests carried out by Skinner (1996) or Birch (1996).

The presence of biotite and phyllosilicates in Alpedrete granite microcracks over the fragmented plagioclase (Figure 5a) could correspond to crystallization of late stage melt that migrated into the opening space. Similar behavior has been reported in other granites (Vernon, 2004).

Details such as the presence of biotite superimposed on microcrack (Figure 5a), bent polysynthetic twins and microcracking of plagioclase parallel and sub-parallel to microcracks indicate some deformation process present in the fresh rock before the treatments.

However, these slight changes and re-accommodation of the minerals; in this granite are specific responses to mechanical stress in plutonic felsitic rocks as reported by Heins (1995). In this regard, the type of deformation is dependent upon the kinds of minerals, interfaces i.e. crystallography and chemistry of adjoining minerals (intercrystalline variations) as well as other crystallographic intracrystalline feature (i.e., twinning planes, zoning patterns, mineral inclusions, etc.). In the case of interfaces, alkaline feldspar, mica and quartz, important advances have been provided by Barber (1990) in respect to the behavior of granite during deformation processes. Aspects including grain size, amount of melt and strain rate may affect the strength and may change the dominant deformation mechanism.

In this case, although relatively few experimental deformation studies have been performed over quartz and feldspar (Barber, 1990), the information of fresh rock is very useful to predict the possible behavior of microcracking of granite feldspar during thermal processes.

The water crystallization in pre-existing microcracks (Freire-Lista et al., 2015a) and thermal expansion of minerals during an accelerated aging tests of the two granites in climatic chambers have created microcracks in K-feldspar and plagioclase. The microcracks propagation mostly following microstructural planes (Přikryl, 2001). As described by Upadhyay (2012), the feldspar microstructure will largely control microcrack propagation which may be inter- or intracrystalline, depending on crystallographic defects or pre-existing microcracks.

Stünitz et al. (2003) observed in plagioclase that dislocations, twinning and deformation bands are interrelated with microcracks to high temperatures (recrystallization). In both Alpedrete and Zarzalejo granites, the intracrystalline microcracks propagate in feldspars following crystallographic planes, cleavage, twins or dislocations. Pseudo-concentric microcracks develop when intracrystalline microcracks propagate following plagioclase zoning. Furthermore, plagioclase crystals have twins and orthogonal cleavage, and in these planes further propagation of microcracks is possible. Microstructural control is different for K-feldspar and plagioclase (Figure 8).

The highest rate of chemical weathering of plagioclase against K-feldspar documented by Taboada and Garcia (1999), is consistent with the increased physical weathering rate found in this study. Plagioclase was subject to more physical decay (microfracturing) than K-feldspar. Svahnberg and Piazzolo (2010) found that the plagioclase core was more susceptible to weathering than its perimeter zone. We observed that in the unstable plagioclase core, where there is more calcium, it is prone to be sericitized (Figure 8) due to granite deuteric alteration and physical disintegration. According to Catlos et al. (2011), zoned plagioclase crystals with a high number of core microcracks is

probably due to controlled thermal expansion. In our study, the higher microcracks number on the plagioclase core was also observed in the granites undergoing FT cycles, so that the propagation and enlargement of pre-existing microcracks communicates plagioclase cores with other areas, which do not always follow cleavage or twin planes. When water within sericitized plagioclase cores freezes, it creates stress and microcrack propagation, increasing the decay due to the weathering.

By comparing the Figures before (Figures 4, 5, 6 and 7) and after (Figure 8) the FT and TS tests it can be seen how in the early stage many of the microcracks are intercrystalline. Also, there is a greater relationship between the oblique microcracks with crystal microstructure. At the end of the tests it was observed that the propagation of fractures had a marked mineral microstructural component.

Sinha and Alsop (2010) observed oblique microcracks propagation to microstructural planes K-feldspar and plagioclase of a granitic mylonite. In studies of microcracks due to uniaxial compression (Rao et al., 2004), the microcracks propagation followed the main compressive stress, regardless of the minerals microstructure. In this study, pressure exerted by ice crystallization or by thermal expansion propagated microcracks whose orientation defined by the microstructure of each mineral. Catlos et al. (2011) indicate that microcrack propagation in granite depends not only on the rock mineralogy, but is also dependent on temperature, pressure of crustal depth and/or degree of interaction with hydrothermal fluids.

The microcracks that were caused by the TS test occur due to differences in thermal expansion coefficients between various minerals and also within the same minerals (Alm et al., 1985; Gorbatshevich, 2003). The rate at which a rock undergoes heat exchange (Shao et al., 2014) and thus the deformation can also influence the spread of microcrack propagation

and increase width of microcracks. In this study microcrack proliferation was faster in the case of TS than for the FT.

The faster decay capacity of the TS test can be explained because each mineral is directly involved in the microcrack generation, which is caused by the volumetric thermal expansibility (e.g., dV/dT ; Skinner, 1966), leading to relevant extent of microcracks and affecting the whole volume of the rock. Considering K-feldspar crystals and plagioclase, more microcracks are generated in plagioclase due to its higher coefficient of thermal expansion (Skinner, 1966). However, the stresses produced by the FT are located in areas where the water has access and can be frozen. These areas are controlled by the primary porosity, which does not affect the whole volume of the rock. Generally, the exposed area is the most microcracked, where water accesses and crystallizes outward (Freire-Lista et al., 2015a) increasing pre-existing microcracks or primary porosity of ashlars.

In this case study, the development of microcracks in both granites have been related to the opening of phyllosilicate crystals (e.g., Suzuki et al., 1995). Thus, in the core of plagioclases occurs alteration to phyllosilicates

such as sericitization. Illite was not detected in our XRD analyses because only K-feldspar was analyzed or illite concentration may be below the detection limits of the tool. However, petrographic studies indicate a high degree of sericitization, without ruling out the presence of expansive clays. For XRD results the presence of local inversion in the maxims diffraction of the AL sample suggests a preferential direction within orthoclase microstructure. These microstructures favor the formation of weaker planes, dislocations and defects facilitating microcrack propagation.

In both of the studied granites pre-existent microcracks and weak crystals orientation are responsible of their anisotropy (Table 1) (Fort et al., 2011). These pre-existing microcracks propagate differently in FT and TS cycles in AL and ZA granites. ZA ends testing with the highest microcracks number in K-feldspar crystals, due to it has higher content of K-feldspar than Plagioclase. Although in relative terms, plagioclase crystals have decay more.

According to Williams et al. (1958) near the margin there is often a tendency for elongated minerals to be aligned with their major axes more or less parallel, so as to produce a distinct

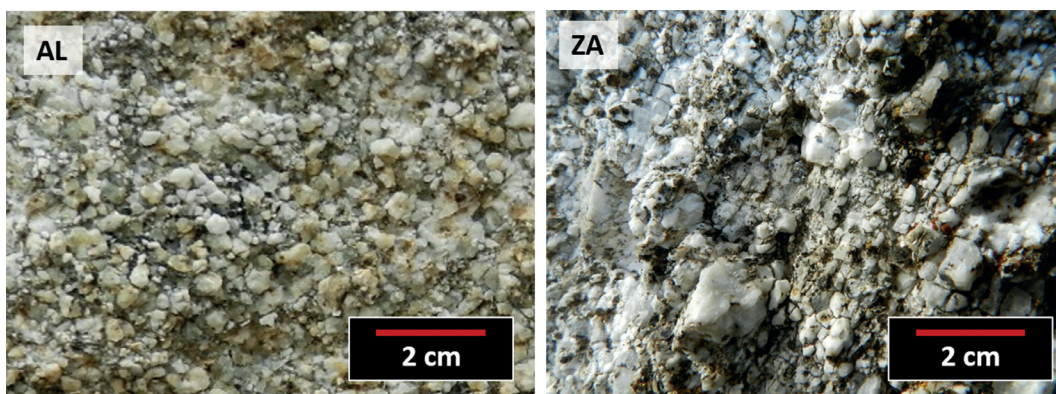


Figure 10. Historical ashlars of altered granite (natural weathering) of AL (Alpedrete granite) and ZA (Zarzalejo granite): microcracks control biological colonization by lichens.

lineation. ZA granite quarries are in an area closest to the pluton margin than AL quarries. Our petrographic results have observed K-feldspar and associated minerals orientation in a ZA granite thin section. According to geological data (Brandebourger, 1984), porphyritic granite textures have been observed in Zarzalejo pluton, which could have affected the reorientation of primary minerals and accessories observed in the thin sections. In addition, in heritage buildings that have used ZA weathered granite (Figure 10) it is possible to see an orientation in their intracrystalline microcracks. This trend is accentuated by the differential decay of minerals, corroborating the findings of this investigation. Similarly, at the end of the test it was observed that microcrack propagation has a marked microstructural component, as it is easier to see this orientation in damaged blocks, than in samples without decay.

Conclusions

Physical weathering caused by artificial thermal processes (FT and TS tests) generated microcrack propagation in K-feldspar and plagioclase crystals, turning them into smaller crystals. ZA crystals are weakly oriented and this petrographical orientation has not been observed in AL. Ice crystallization resulting from freeze-thaw testing in pre-existing microcracks and volumetric expansion of minerals as a result of thermal shock test produce stresses in K-feldspar and plagioclase crystals that propagate microcracks inherent in weaker microstructural planes. Microcracking of feldspars produces crystal loss on the granite surface and allows other chemical alteration processes to occur predisposing them to weathering by fluid flow or air pollutants. This accelerates the decay process causing the formation of black crusts, and biodeterioration by biological colonization (e.g., lichens and plants), among others.

Stress is located in the pre-existing microcracks

and they propagate by crystallographic weaknesses planes, communicating pre-existing microcracks. Microscopic analysis of microcracks versus microstructure feldspars enhances understanding microcrack propagation of the feldspars. TS test had further granite decay action than FT test. The granite most affected by feldspar microcrack propagation was ZA.

Acknowledgements

This study was funded by the Community of Madrid under the GEOMATERIALS 2 project (S2013/MIT-2914). The authors are members of the Complutense University of Madrid's Research Group: "Alteración y Conservación de los Materiales Pétreos del Patrimonio" (ref. 921349). The authors wish to thank the Geological and Mining Institute of Spain for conducting the thermal shock tests. The petrophysical assessments were run at the IGEO Petrophysical Laboratory, affiliated with the Moncloa Campus of International Excellence (UCM-UPM) Heritage Laboratory Network (RedLabPat).

The authors thank Mark Wass, English native speaker, for his help in editing this work and anonymous reviews, their comments have been very helpful to improve the paper quality.

References

- Alm O, Jaklund L.L. and Kou S. (1985) - The influence of microcrack density on the elastic and fracture mechanical properties of Stripa granite. *Physics of the Earth and Planetary Interiors*, 40 (3), 161-179.
- Anders M.H., Laubach S.E. and Scholz C.H. (2014) - Micromicrocracks: A review. *Journal of Structural Geology*, 69, 377-394.
- Akagawa S. and Fukuda M. (1991) - Frost heave mechanism in welded tuff. *Permafrost and Periglacial Processes*, 2, 301-309.
- Åkesson U., Hansson J. and Stigha J. (2004) - Characterisation of microcracks in the Bohus granite, western Sweden, caused by uniaxial cyclic

- loading. *Engineering Geology*, 72, 131-142.
- Barber D.J. and Meredith P.O. (1990) - Deformation processes in minerals, ceramics and rocks. London, Unwin Hyman, 423 pp.
- Bard J.P. (1986) - Microtextures of Igneous and Metamorphic Rocks. D. Reidel Publishing Company, Dordrecht, Holland, Softcover reprint of the hardcover 1st edition, 264 pp.
- Brandebourger E. (1984) - Les granitoides Hercyniens tardifs de la Sierra de Guadarrama Systeme Central Espagne. Petrographie et geochemie. Ph.D Thesis, Universite Lorraine, 209 pp.
- Bayram F. (2012) - Predicting mechanical strength loss of natural stones after freeze-thaw in cold regions. *Cold Regions Science and Technology*, 83-84, 98-102.
- Bernabéu A., Benavente D., Fort R., García del Cura M.A., Martínez-Martínez J. and Mendiña J. (2004) - Valoración petrofísica del granito de Zarzalejo (Sistema Central) para su utilización como piedra de pavimento en cascos históricos. 6^o Reunión Red Temática de Patrimonio Histórico y Cultural. CSIC. Seville, Centro Nacional de Aceleradores.
- Birch F. (1996) - Compressibility; elastic constant. *Geological Society of America memoir*, 97, 97-173.
- Borrelli L., Perri F., Critelli S. and Gullà G. (2012) - Mineropetrographical features of weathering profiles in Calabria, southern Italy. *Catena*, 92, 196-207.
- Caracciolo L., Tolosana-Delgado R., Le Pera E., von Eynatten H., Arribas J. and Tarquini S. (2012) - Influence of granitoid textural parameters on sediment composition: Implications for sediment generation. *Sedimentary Geology*, 280, 93-107.
- Çatlos E., Baker C., Sorensen S., Jacob L. and Çemen I. (2011) - Linking microcracks and mineral zoning of detachment-exhumed granites to their tectonomagmatic history: Evidence from the Salihli and Turgutlu plutons in western Turkey (Menderes Massif). *Journal of Structural Geology*, 33, 951-969.
- Chen Y., Kobayashi T., Kuriki Y., Kusuda H. and Mabuchi M. (2008) - Observation of microstructures in granite samples subjected to one cycle of heating and cooling. *Journal of the Japan Society of Engineering Geology*, 49(4), 217-26.
- Eggleton R.A. and Buseck P.R. (1980) - High resolution electron microscopy of feldspar weathering. *Clays and Clay Minerals*, 28, 173-178.
- European Standard EN 12371 (2001) - Natural stone test methods-Determination of frost resistance.
- European Standard EN 14066 (2003) - Natural stone test methods - Determination of resistance to ageing by thermal shock.
- Fort R., Alvarez de Buergo M., Perez-Monserrat E. and Varas M.J. (2010) - Monzogranitic batholiths as a supplying source for the heritage construction in the northwest of Madrid. *Engineering Geology*, 115, 149-157. DOI:10.1016/j.enggeo.2009.09.001.
- Fort R., Varas M.J., Alvarez de Buergo M. and Freire-Lista D.M. (2011) - Determination of anisotropy to enhance the durability of natural stone. *Journal of Geophysics and Engineering*, 8, 132-144.
- Fort R., Alvarez de Buergo M., Perez-Monserrat E., Gómez-Heras M., Varas M.J. and Freire-Lista D.M. (2013) - Evolution in the use of natural building stone in Madrid, Spain. *Quarterly Journal of Engineering Geology and Hydrogeology*, 46, 421-429.
- Franzoni E., Sassonia E., Scherer G.W. and Naidu S. (2013) - Artificial weathering of stone by heating. *Journal of Cultural Heritage*, 14s, 85-93.
- Freire-Lista D.M. and Fort R. (2015) - The region of the Piedra Berroqueña: A potencial Global Heritage Stone Province. Geophysical Research Abstracts, EGU General Assembly, 3047.
- Freire-Lista D.M., Fort R. and Varas-Muriel M.J. (2015a) - Freeze-thaw fracturing in building granites. *Cold Regions Science and Technology*, 113, 40-51. DOI: 10.1016/j.coldregions.2015.01.008.
- Freire-Lista D.M., Fort R. and Varas-Muriel M.J. (2015b) - Alpedrete granite (Spain). A nomination for the "Global Heritage Stone Resource" designation. *Episodes*, 38 (2), 1-8.
- García-del-Cura M.A., Benavente D., Bernabéu A., and Martínez-Martínez J. (2008) - The effect of surface finishes on outdoor granite and limestone pavers. *Materiales de Construcción* 58, 289-290, 65-79, ISSN: 0465-2746 e ISSN: 1988-3226.
- Gómez-Heras M., Smith B. J. and Fort R. (2006) - Surface temperature differences between minerals in crystalline rocks: implications for granular disintegration of granites through thermal fatigue. *Geomorphology*, 78, 236-249.
- Gómez-Heras M., Smith B. J. and Fort R. (2008) - Influence of surface heterogeneities of building granite on its thermal response and its potential for the generation of thermoclasty. *Environmental Geology*, 56, 547-560.
- Gómez-Heras M., Stephen M., Smith B. J. and Fort R. (2009) - Impacts of Fire on Stone-Built Heritage. An

- Overview. *Architectural Conservation*, 2, 15, 47-58.
- Gorbatsevich F.F. (2003) - Decompression mechanism of deep crystalline rocks under stress relief. *Tectonophysics*, 370, 121-128.
- Gräf V., Jamek M., Rohatsch A. and Tschegg E. (2013) - Effects of thermal-heating cycle treatment on thermal expansion behavior of different building stones. *Rock Mechanics & Mining Sciences*, 64, 228-235.
- Hall K. and Thorn E. (2014) - Thermal fatigue and thermal shock in bedrock: An attempt to unravel the geomorphic processes and products. *Geomorphology*, 206, 1-13.
- Hallet B., Walder J.S. and Stubbs C.W. (1991) - Weathering by segregation ice growth in microcracks at sustained subzero temperatures: Verification from an experimental study using acoustic emissions. *Permafrost and Periglacial Processes*, 2, 283-300.
- Heins W.A. (1995) - The use of mineral interfaces in sand-sized rock fragments to infer ancient climate. *Geological Society of America Bulletin* 107, 113-125.
- Hor M. and Morihiro H. (1998) - Micromechanical analysis on deterioration due to freezing and thawing in porous brittle materials. *International Journal of Engineering Sciences*, 36 (4), 511-522.
- Ingham J.P. (2005) - Predicting the frost resistance of building stone. *Quarterly Journal of Engineering Geology and Hydrogeology*, 38, 387-399.
- Insera C., Biwa S. and Chen Y. (2013) - Influence of thermal damage on linear and non linear acoustic properties of granite. *International Journal of Rock Mechanics and Mining Sciences*, 62, 96-104.
- Iñigo A.C., Vicente M.A., and Rives V. (2000) - Weathering and decay of granitic rocks: its relation to their pore network. *Mechanics of Materials*, 32, 555-560.
- Iñigo A.C., García-Talegón J., Vicente-Tavera S., Martín-González S., Casado-Marín S., Vargas-Muñoz M. and Pérez-Rodríguez J.L. (2013) - Colour and ultrasound propagation speed changes by different ageing of freezing/thawing and cooling/heating in granitic materials. *Cold Regions Science and Technology*, 85, 71-78.
- Iversen E. (1992) - The heritage of Ancient Egypt. Copenhagen, G.E.C. Gad, 123 pp.
- Jamshidi A., Reza-Nikudel M., Nikudel and Khamehchiyan M. (2013) - Predicting the long-term durability of building stones against freeze-thaw using a decay function model. *Cold Regions Science and Technology*, 92, 29-36.
- Kanagawa K., Shimano H. and Hiroi Y. (2008) - Mylonitic deformation of gabbro in the lower crust: a case study from the Pankenushi gabbro in the Hidaka metamorphic belt of central Hokkaido, Japan. *Journal of Structural Geology*, 30, 1150-1166.
- Kranz R.T. (1983) - Microcracks in rocks: a review. *Tectonophysics*, 100, 449-480.
- Lee M.R. and Parsons I. (1995) - Microtextural controls of weathering of perthitic alkali feldspars. *Geochimica et Cosmochimica Acta*, 59 (21) 4465-4488.
- Le Pera E. and Sorriso-Valvo M. (2000) - Weathering and morphogenesis in a Mediterranean climate, Calabria, Italy. *Geomorphology*, 34, 251-270.
- Lin W., Takahashi M. and Sugita N. (1995) - Change of microcrack widths induced by temperature increase in Inada granite. *Journal of the Japan Society of Engineering Geology*, 36, 300-304.
- Lin W. (2002) - Permanent strain of thermal expansion and thermally induced microcracking in Inada granite. *Journal of geophysical research*, 107, NO. B10, 2215, DOI: 10.1029/2001JB000648.
- López-Arce P., Varas-Muriel M.J., Fernández-Revuelta B., Álvarez de Burgos M., Fort R. and Pérez-Soba C. (2010) - Artificial weathering of Spanish granites subjected to salt crystallization tests: surface roughness quantification. *Catena*, 83, 170-185.
- McLaren A.C. and Pryer L.L. (2001) - Microstructural investigation of the interaction and interdependence of cataclastic and plastic mechanisms in Feldspar crystals deformed in the semi-brittle field. *Tectonophysics*, 335, 1-15.
- Malaga-Starzec K., Åkesson U., Lindqvist J.E. and Schouenborg B. (2006) - Microscopic and macroscopic characterization of the porosity of marble as a function of temperature and impregnation. *Construction and Building Materials*, 20, 939-947.
- Martínez-Martínez J., Benavente D., Gómez-Heras M., Marco-Castaño L. and García-del-Cura M.A. (2013) - Non-linear decay of building stones during freeze-thaw weathering processes. *Construction and Building Materials*, 38, 443-454.
- Matsuoka N. and Murton J. (2008) - Frost Weathering: Recent Advances and Future Directions. *Permafrost and Periglacial Processes*, 19, 195-210.
- Mehl L. and Hirth G. (2008) - Plagioclase preferred orientation in layered mylonites: evaluation of flow laws for the lower crust. *Journal of Geophysical Research*, 113, B05202. DOI: 10.1029/2007JB005075.

- Menduiña J., and Fort R. (coordinadors) (2005) - Las piedras utilizadas en la construcción de los Bienes de Interés Cultural de la Comunidad de Madrid anteriores al siglo XIX. IGME-IGE, Madrid, 131 pp.
- Mills K. (1991) - Metals handbook: Fractography American Society of Metals, Asm International, OHIO, 517 pp.
- Michel-Lévy A. (1894) - Etude sur la détermination des feldspaths dans les plaques minces au point de vue de la classification des roches. Librairie Polytechnique, Baudry et Cie, Paris, 108 pp. + 18 pp.
- Ollier C.D. (1983) - Weathering or hydrothermal alteration? *Catena*, 10, 57-59.
- Ozcelik Y., Careddu N. and Yilmazkaya E. (2012) - The effects of freeze-thaw cycles on the gloss values of polished stone surfaces. *Cold Regions Science and Technology*, 82, 49-55.
- Page R. and Wenk H.R. (1979) - Phyllosilicate alteration of plagioclase studied by transmission electron microscopy. *Geology*, 7, 393-397.
- Pires V., Rosa L.G. and Dionisio A. (2014) - Implications of exposure to high temperatures for stone cladding requirements of three Portuguese granites regarding the use of dowel-hole anchoring systems. *Construction and Building Materials*, 201 (64), 440-450.
- Přikryl R. (2001) - Some microstructural aspects of strength variation in rocks. *International Journal of Rock Mechanics & Mining Sciences*, 38, 671-682.
- Rao M.V.M.S., Murthy D.S.N., Rao G.M.N., Mohanty S.K. and Udayakumar S. (2004) - Stress-induced micro-cracking and brittle failure of Godhra Granite, Gujarat: a laboratory investigation using acoustic emission. *Journal of the Geological Society of India*, 64, 775-783.
- Reuschlé T., Haore S.G. and Darot M. (2003) - Microstructural control on the elastic properties of thermally cracked granite. *Tectonophysics*, 370, 95-104.
- Reuschlé T., Haore S.G. Darot M. (2006) - The effect of heating on the microstructural evolution of La Peyratte granite deduced from acoustic velocity measurements. *Earth and Planetary Science Letters*, 243, 692-700.
- Scarciglia F., Le Pera E. and Critelli S. (2005) - Weathering and pedogenesis in the Sila Grande Massif (Calabria, South Italy): from field scale to micromorphology. *Catena*, 61, 1-29.
- Scarciglia F., Saporito N., La Russa M.F., Le Pera E., Macchione M., Puntillo D., Crisci G.M. and Pezzino A. (2012) - Role of lichens in weathering of granodiorite in the Sila uplands (Calabria, southern Italy). *Sedimentary Geology*, 280, 119-134.
- Schouenborg B.E. (1996) - Frost resistance of natural stones in the nordic countries. Proceeding of the seventh international conference, London, 1091-1100.
- Seo Y.S., Jeong G.C., Kim J.S. and Ichikawa Y. (2002) - Microscopic observation and contact stress analysis of granite under compression. *Engineering Geology*, 63, 259-275.
- Shao S., Wasantha P.L.P., Ranjith P.G. and Chen B.K. (2014) - Effect of cooling rate on the mechanical behavior of heated Strathbogie granite with different grain sizes. *International Journal of Rock Mechanics and Mining Sciences*, 70, 381-387.
- Skinner B.J. (1966) - Thermal expansion. In Handbook of physical constants. *Geological Society of America Memoirs*, 97, 75-96.
- Sinha S., Alsop G.I. and Biswal T.K. (2010) - The evolution and significance of microfracturing within feldspars in low-grade granitic mylonites: A case study from the Eastern Ghats Mobile Belt, India. *Journal of Structural Geology*, 32, 1417-1429.
- Smith J.V. (1974) - Feldspar minerals, Chemical and Textural Properties, Springer-Verlag Berlin Heidelberg New York, 2, 692 pp.
- Sousa L.M.O., Suárez del Río L.M. and Calleja L., Ruiz de Argandoña V.G. and Rodríguez A. (2005) - Influence of microfractures and porosity on the physico-mechanical properties and weathering of ornamental granites. *Engineering Geology*, 77, 153-168.
- Sousa L.M.O. (2014) - Petrophysical properties and durability of granites employed as building stone: a comprehensive evaluation. *Bulletin of Engineering Geology and the Environment*, 73, 569-588.
- Stoch L. and Sikora W. (1976) - Transformation of micas in the process of kaolinization of granites and gneiss. *Clays and Clay Minerals*, 24, 156-162.
- Stünitz H., Fitz Gerald J.D. and Tullis J. (2003) - Dislocation generation, slip systems and dynamic recrystallization in experimentally deformed plagioclase single crystals. *Tectonophysics*, 372, 215-233.
- Suzuki K., Oda M., Kuwahara T. and Hiram K. (1995) - Material property changes in granitic rock during long-term immersion in hot water. *Engineering*

- Geology*, 40 29-39.
- Svahnberg H. and Piazzolo S. (2010) - The initiation of strain localization in plagioclase-rich rocks: Insights from detailed microstructural analyses. *Journal of Structural Geology*, 32, 1404-1416.
- Tabbakh Shabani A.A. (2009) Mineral Chemistry of Chlorite Replacing Biotite from Granitic Rocks of the Canadian Appalachians. *Journal of Sciences, Islamic Republic of Iran*, 20(3), 265-275 <http://jsciences.ut.ac.ir>, University of Tehran, ISSN 1016-1104.
- Taboada T. and García C. (1999) - Pseudomorphic transformation of plagioclases during the weathering of granitic rocks in Galicia NW Spain. *Catena*, 35, 291-302.
- Takarli M., Prince W. and Siddique R. (2008) - Damage in granite under heating/cooling cycles and water freeze-thaw conditions. *International Journal of Rock Mechanics and Mining Sciences*, 45, 1164-1175.
- Tan X., Chen W., Yang J. and Cao J. (2011) - Laboratory investigations on the mechanical properties degradation of granite under freeze-thaw cycles. *Cold Regions Science and Technology*, 68, 130-138.
- Tullis J. and Yund R.A. (1985) - Dynamic recrystallization of feldspar: a mechanism for ductile shear zone formation. *Geology*, 13, 238-241.
- Tullis J. and Yund R.A. (1987) - Transition from cataclastic flow to dislocation creep of feldspar: mechanisms and microstructures. *Geology*, 15, 606-609.
- Tullis J. and Yund R.A. (1992) - The brittle-ductile transition in feldspar aggregates: an experimental study. In: Evans, B., Wong, T.F (Eds.), *Fault Mechanics and Transport Properties in Rocks*. Academic Press, New York, 89-118.
- Hadizadeh J. and Tullis J. (1992) - Cataclastic flow and semi-brittle deformation of anorthosite. *Journal of Structural Geology*, 14, 57-63.
- Upadhyay D. (2012) - Alteration of plagioclase to nepheline in the Khariar alkaline complex, SE India: Constraints on metasomatic replacement reaction mechanisms. *Lithos*, 155, 19-29.
- Vázquez P., Alonso F.J. Esbert R.M. and Ordaz J. (2010) - Ornamental granites: Relationships between p-waves velocity, water capillary absorption and the crack network. *Construction and Building Materials*, 24, 2536-2541.
- Vázquez P., Shushakova V. and Gómez-Heras M. (2015) - Influence of mineralogy on granite decay induced by temperature increase: Experimental observations and stress simulation. *Engineering Geology*, 189, 58-67.
- Vernon R.H. (2004) - A practical guide to rock microstructure, Cambridge University Press, ISBN 978-0-521-89133-2.
- Villaseca C., Barbero L. and Rogers G. (1998) - Crustal origin of Hercynian peraluminous granitic batholiths of Central Spain: petrological, geochemical and isotopic (Sr, Nd) constraints. *Lithos*, 43(2), 55-79.
- Villaseca C. and Herreros V. (2000) - A sustained felsic magmatic system: the Hercynian granitic batholith of the Spanish Central System. Transactions of the Royal Society of Edinburgh. *Earth Sciences*, 91, 207-219.
- Walder J. and Hallet B. (1985) - A theoretical model of the fracture of rock during freezing. *Geological Society of America Bulletin*, 96, 336-346.
- Williams H., Turner F. and Gilbert Ch. (1958) - An introduction to the study of rocks in thin sections. W.H. Freeman and company. 406 pp.
- Wilson M.J. (2004) - Weathering of the primary rock-forming minerals: processes, products and rates. *Clay Minerals*, 39, 233-266.

Submitted, February 2015 - Accepted, July 2015